

Microcrack accumulation at different intervals during fatigue testing of compact bone

Fergal J. O'Brien^{a,b,*}, David Taylor^b, T. Clive Lee^{a,b}

^aDepartment of Anatomy, Royal College of Surgeons in Ireland, St Stephen's Green, Dublin 2, Ireland

^bDepartment of Mechanical and Manufacturing Engineering, Trinity College, Dublin 2, Ireland

Accepted 28 January 2003

Abstract

Fatigue damage in bone occurs in the form of microcracks. This microdamage contributes to the formation of stress fractures and acts as a stimulus for bone remodelling. A technique has been developed, which allows microcrack growth to be monitored during the course of a fatigue test by the application of a series of fluorescent chelating agents. Specimens were taken from bovine tibiae and fatigue tested in cyclic compression at a stress range of 80 MPa. The specimens were stained before testing with alizarin and up to three other chelating agents were applied during testing to label microcracks formed at different times. Microcracks initiated in interstitial bone in the early part of a specimen's life. Further accumulation of microcracks is then suppressed until the period late in the specimen's life. Microcracks were found to be longer in the longitudinal than in the transverse direction. Only a small proportion of cracks are actively propagating; these are longer than non-propagating cracks. These results support the concept of a microstructural barrier effect existing in bone, whereby cracks initiate easily but slow down or stop at barriers such as cement lines. © 2003 Elsevier Science Ltd. All rights reserved.

Keywords: Microcrack; Propagation; Accumulation; Osteon; Barrier

1. Introduction

Fatigue damage in a bone acts as a stimulus for bone remodelling (Martin and Burr, 1982; Burr et al., 1985; Burr and Martin, 1993; Mori and Burr, 1993; Prendergast and Taylor, 1994; Lee and Taylor, 1999; Martin, 2000). Bones, therefore, have an advantage over most engineering structures in that they have an inherent ability to repair damage. However, if this damage accumulates at such a rate that the capacity for bone repair is exceeded, stress fractures result. These fractures occur commonly in athletes and soldiers engaged in high intensity, repetitive activities such as marching or running. If, on the other hand, damage accumulates at 'normal' rates but the bone's repair mechanism is deficient, fragility fractures result, which

occur commonly in ageing bone (Schaffler et al., 1994a, 1995).

The resistance of any material to fatigue failure is a function of its resistance to either or both the initiation and propagation of cracks. Osteonal bone can be compared to composite materials and to metals whereby discontinuities within the material (e.g. fibres, laminae, voids) may provide stress concentration sites for crack initiation, but they also serve as barriers to crack growth which may slow down or even halt crack propagation. Some authors have mentioned the possibility of a microstructural barrier concept existing in bone (Martin and Burr, 1989; Taylor and Prendergast, 1997; Taylor, 1998; Akkus and Rinnac, 2001), whereby the critical stage in the fatigue process is not the initiation of cracks but their propagation beyond microstructural sizes.

The cement line interface between osteons and interstitial bone is relatively weak which means that it may reduce the shear strength of osteonal bone (Frasca, 1981). However slipping at this interface relaxes shear stresses, reduces strain energy and slows crack propagation. Park and Lakes (1986) studied the viscoelastic creep behaviour of human bone and found experimental

*Corresponding author. Department of Materials Science and Engineering, Massachusetts Institute of Technology, 77 Massachusetts Avenue, Cambridge, MA 02139, USA. Tel.: +1-617-253-2076; fax: +1-617-258-6275.

E-mail address: fjobrien@mit.edu (F.J. O'Brien).

evidence which suggested that the osteonal cement line only fails after other damage has accumulated in the bone matrix. Jepsen et al. (1999) showed that the lamellar interface in bone is weak and is the principal site of shear damage formation but the lamellar interface was shown to be highly effective in keeping cracks isolated from each other. Zioupos et al. (1994) showed that microcracks in bone did interact with the microstructure of the bone and that the grain of the bone constrained their growth directions. They hypothesised that the presence of lamellae influenced the process by which microcracks coalesced but that vascular or other naturally occurring cavities did not initiate microcracking and appeared to deflect microcracks. Schaffler et al. (1994b) used back-scattered electron microscopy on fuchsin stained sections of human rib to show that features of the bone matrix ultrastructure, such as the collagen fibre-bone mineral relationship play a key role in minimising the formation of larger detrimental cracks whilst encouraging the formation of numerous small cracks which do not propagate as readily to failure. Boyce et al. (1998) showed experimentally that microcracks developed in the interstitial tissue regions and stopped at the osteonal boundaries, while Schaffler et al. (1995) added quantitative data to this hypothesis suggesting that 80–90% of all microcracks in cortical bone are found in the interstitial matrix between osteons.

Fatigue damage in bone occurs in the form of microcracks. Little work has been carried out to look at the process of damage accumulation during a fatigue test. In attempting to understand the process, other authors have performed fatigue tests, stopping the tests prior to failure to allow histological analysis of damage developed before fracture. Burr et al. (1998) carried out four point bending tests on whole canine femurs and found increases in crack numerical density and crack surface density, accompanied by decreases in elastic modulus. Forwood and Parker (1989) loaded rat tibiae in torsion at different strain levels. They found increasing microdamage accumulation in response to increased loading. They also found that many microcracks crossing the bone cortex were arrested by osteons but that at the highest level of loading, the deformation applied was sufficient to drive the cracks through the full thickness of the bone cortex. Akkus and Rimnac (2001) looked at the propagation and growth of individual microcracks under uniaxial tension. They found that the growing microcracks initially slowed down, either arresting or passing through a minimum growth rate before accelerating. Their results support the concept of a microstructural barrier effect for cortical bone tissue. The limitations of their work include the fact that they only looked at surface cracks and also disregarded microcracks that did not run in straight lines, and they did not look at the actual mechanisms by which microcrack

growth was arrested. Despite these previous studies, the process by which fatigue microcracks in bone initiate and grow remains poorly understood and little work has been carried out to show at what periods during a test microcracks initiate, accumulate and ultimately bring about failure. This work seeks to redress the problem. A technique has been developed (Lee et al., 2000a,b; O'Brien et al., 2002) which allows microcrack growth to be monitored during the course of a mechanical fatigue test by the application of a series of fluorescent chelating agents. By using this technique, it is proposed to obtain more information on the behaviour of microcracks and their influence on the fatigue life of bone.

Objectives

1. To monitor microdamage accumulation at different stages during a specimen's life by the application of a series of fluorescent chelating agents at intervals during a fatigue test.
2. To record the numbers and lengths of microcracks during different stages of the specimen's life.
3. By sectioning failed specimens both transversely and longitudinally, to examine the crack shape and size and to monitor how this changes during testing.
4. To study the influence of bone microstructure on the propagation of microcracks especially the role of osteons and their cement lines.
5. To compare the behaviour of pre-existing microcracks with those which initiate during testing.

2. Materials and methods

Samples of cortical bone were removed from the mid-diaphyses of 17 bovine tibiae and machined into standard sized test specimens consistent with earlier work in this laboratory (Taylor et al., 1999; Lee et al., 2000b). Testing was carried out in an INSTRON 8501 servo-hydraulic testing machine used in load control to apply an axial compressive force to the specimens, which were enclosed in a small plastic bath to which the dyes could be added. All tests were carried out at room temperature, at a frequency of 3 Hz, with a stress range of 80 MPa and a ratio between minimum and maximum stress of 0.1. Specimens were kept wet during all stages of machining and testing.

Specimens were removed from the freezer on the day prior to testing, allowed to thaw and placed in a single vial of 0.0005 M alizarin in a dessicator at 50 mm Hg vacuum for 16 h to label any microdamage which existed prior to testing. A pre-determined sequence of dyes (Lee et al., 2000b; O'Brien et al., 2002) was used as shown in Table 1. Dyes were changed after 10,000 and 50,000 cycles as these represented approximately 10% and 50% of total life. Specimens were rinsed in distilled water before each change of dye to ensure that all of the

Table 1
Sequence of application of chelating agents

Agent	Colour	Excitation wavelength (nm)	Period of application	
			3 agent tests	4 agent tests
Alizarin	Red	375	Prior to test	Prior to test
Xylenol	Orange	377	First 50,000 cycles	First 10,000 cycles
Calcein	Green	495	50,000 cycles to failure	10,000 to 50,000cycles
Calcein blue	Sky blue	580	Not used	50,000 cycles to failure

preceding dye was removed. Failure was defined using established criteria; a 10% reduction in stiffness (Taylor et al., 1999) which generally coincided with the appearance of a large crack. Ten tests were carried out with three agents applied and having established that the sequential labelling technique worked successfully, a further three tests were conducted with a fourth agent included (see Table 1).

Following testing, the gauge length of the specimens was removed using a diamond saw (Struers Miniton), divided into two sections, and randomly assigned for analysis of longitudinal sections or transverse sections. Sections 250 μm thick were cut, handground to between 100 and 150 μm and mounted under a glass coverslip. They were examined using epifluorescence microscopy, their cross-sectional areas obtained and microcracks identified and measured using the established criteria (Lee et al., 2000a, b; O'Brien et al., 2000). Fig. 1 shows an example of a microcrack viewed using (a) green epifluorescence ($\lambda = 546 \text{ nm}$) and (b) UV epifluorescence ($\lambda = 365 \text{ nm}$). The results were tabulated in the form of: numerical crack density—Cr.Dn (number of cracks occurring per mm^2); surface crack density—Cr.S.Dn (total μm of crack/ mm^2); and mean crack length—Cr. Le. Cracks in transverse sections were also described in terms of location, i.e., osteonal, where they were located entirely within a secondary osteon or traversed a cement line surrounding a secondary osteon, and interstitial: where they were located completely in interstitial bone between osteons or in cement lines.

The classification system defined microcracks labelled with alizarin as pre-existing. Following the fatigue tests, three further bone samples were used in order to establish how many of these cracks existed prior to machining and were in vivo microcracks and how many were microcracks formed by the coring and lathing process. Three samples of bone were removed from the mid-diaphysis of three bovine tibiae using the same technique as had been used for the test specimens. Each sample was placed in a single vial of 0.0005 M alizarin in a dessicator at 50 mm Hg vacuum for 16 h to label microdamage which was formed in vivo. Ground sections were then made and the sections were analysed for microcracks. During the analysis process any microcracks found within 500 μm of the bone surface

were ignored, so as to prevent any cracks formed by the bandsaw being counted.

In all specimens, one observer identified microcracks and it was estimated from a number of preliminary tests that the lower limit for reliable crack detection was a length of 30 μm , errors in measured length were in the range of $\pm 10 \mu\text{m}$, and errors in length change for propagating microcracks were in the range of $\pm 20 \mu\text{m}$. Unpaired *t*-tests with a probability value of 95% ($p < 0.05$) were used to analyse the data.

3. Results

The mean number of cycles to failure was 88,380 (S.D. 22,400) ($n = 13$). When the data from the four agent tests was compared to the equivalent data from the three agent tests, the results were found to be comparable and differences were not statistically significant ($p > 0.05$), so the two sets of data were accumulated for subsequent analysis. Tables 2 and 3 show the data obtained; propagating microcracks are defined as cracks which were labelled with two or more agents. Fig. 2 shows the variation of microcrack densities, Cr.Dn and Cr.S.Dn as a function of the number of cycles. Failure is defined as the mean number of cycles to failure from all the tests. These plots show that microcracks developed rapidly in the first 10,000 cycles but microcrack density did not increase significantly again until after 50,000 cycles had elapsed.

Transverse sections were found to have a greater Cr.Dn value than longitudinal sections by almost a factor of 2 on average, when cracks at all stages during testing were considered ($p < 0.05$). The mean Cr.Dn for pre-existing transverse microcracks was 0.036 ± 0.028 cracks/ mm^2 and for pre-existing longitudinal microcracks was 0.018 ± 0.024 cracks/ mm^2 and these did not propagate during testing. Only 8% of all microcracks were labelled with two or more agents showing that they had propagated during testing. These propagating microcracks were measured prior to failure, cracks formed by the propagation of the main failure crack were not quantified. Fig. 3 shows an example of a propagating microcrack which is labelled with xylenol orange and calcein.

When microcracks at all stages of a specimen's life were analysed together, microcracks were found to be longer in longitudinal than in transverse sections by a factor of 2.25 ($p < 0.05$). Pre-existing microcracks were short in comparison to the other types (transverse: $52 \mu\text{m}$ S.D. $35 \mu\text{m}$; longitudinal: $67 \mu\text{m}$ S.D. $45 \mu\text{m}$) ($p < 0.05$) and in general were found close to the surface of the specimen. No significant difference in length was found between non-propagating microcracks which

were formed at different periods of a test. Propagating microcracks were longer than the other types of microcracks (transverse: $231 \mu\text{m}$ S.D. $106 \mu\text{m}$; longitudinal: $331 \mu\text{m}$ S.D. $132 \mu\text{m}$); no cracks were found which had been labelled with more than two agents, and no cracks were found which had been labelled with the same agent twice, i.e. labelled in different regions of the same microcrack with the same chelating agent, indicating that propagation did not take place from both ends of a microcrack. This was found for both

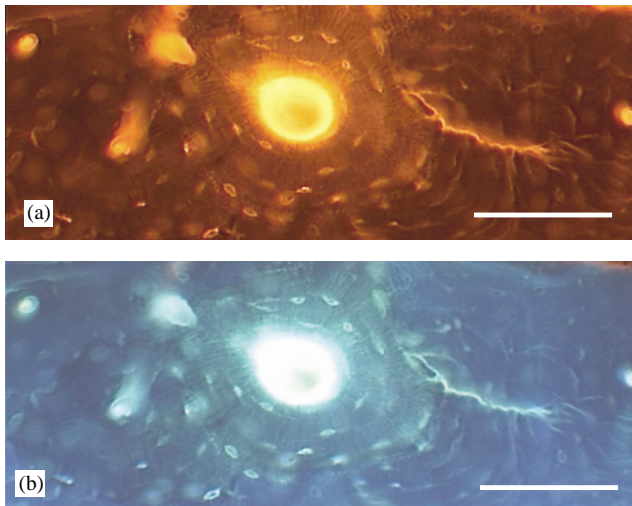


Fig. 1. Calcein labelled microcrack viewed using (a) green epifluorescence ($\lambda = 546 \text{ nm}$) and (b) UV epifluorescence ($\lambda = 365 \text{ nm}$). This microcrack is located in interstitial bone but part of it is found on the perimeter of a cement line surrounding a Haversian system.

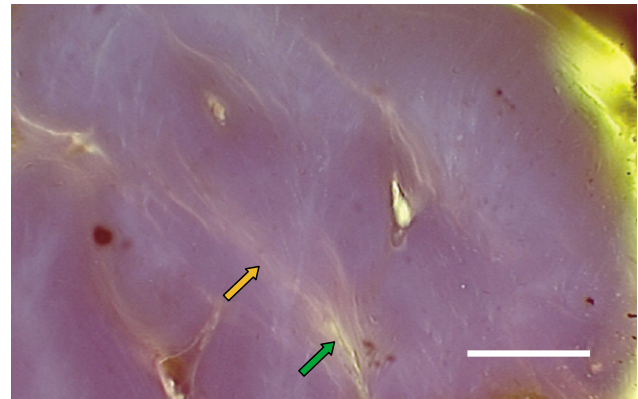


Fig. 3. Example of propagating microcrack, initially stained with xylenol (orange arrow) and then stained with calcein (green arrow) showing it, to have been formed during the first 50,000 cycles and then to have grown further between 50,000 cycles and failure. Other xylenol orange labelled microcracks can also be seen in the image. Bar = $100 \mu\text{m}$.

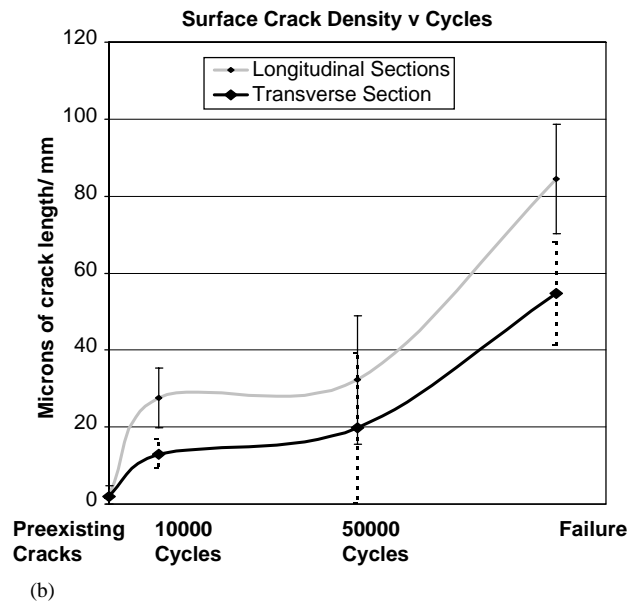
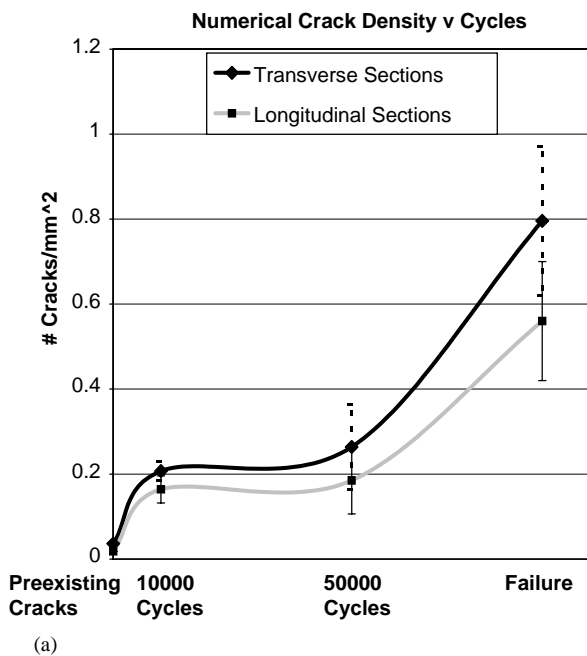


Fig. 2. Microcrack accumulation during the course of testing (a) Cr.Dn versus time (b) Cr.S.Dn versus time. These figures show total accumulated crack densities when the time period indicated had elapsed, i.e.: the densities at failure indicate the sum of pre-existing, propagating and microcracks which formed within individual time periods. Both graphs show a similar trend, microcrack density increases rapidly during the first 10,000 cycles but then there is a reduced rate of accumulation until 50,000 cycles have elapsed after which there is another rapid rate of accumulation.

propagating microcracks in interstitial bone and those found within osteons. No microcracks that formed within the first 10,000 cycles of testing were found to propagate.

Fig. 4 shows the distribution of microcracks from transverse sections by location. Microcrack location in longitudinal sections was not analysed owing to difficulties in identifying cement lines in these sections. The significant majority of all microcracks were found in interstitial bone and did not enter secondary osteons ($p < 0.05$). For microcracks formed in the first 50,000 cycles, 91% of them were located in interstitial bone and although this figure drops for microcracks formed after

50,000 cycles of a test had elapsed less than 25% of them were located in osteons. Table 4 shows the results from the control study comparing machine induced to in vivo microcracks. It was found that machine-induced cracks outnumbered in vivo cracks by a factor of 2.5. Only one out of 54 pre-existing microcracks was found to propagate during testing.

4. Discussion

The chelating agents allowed a clear distinction to be made between microcracks formed at different stages

Table 2
Crack data obtained from transverse sections from all tests

Crack type	Pre-existing	First 10,000 cycles	10,000 to 50,000 cycles	50,000 cycles to failure	Propagating
Cr.Le (μm)	51.6	99.0	101	118.5	231.4
S.D.	35.1	43.8	16.1	78.9	106.5
Cr.Dn (No./ mm^2)	0.036	0.171	0.057	0.532	0.049
S.D.	0.028	0.023	0.048	0.175	0.084
Cr.S.Dn ($\mu\text{m}/\text{mm}^2$)	1.87	11.12	6.79	35.01	7.53
S.D.	0.39	3.73	21.4	13.3	13.62

Table 3
Crack data obtained from longitudinal sections from all tests

Crack type	Pre-existing	First 10,000 cycles	10,000–50,000 cycles	50,000 cycles to failure	Propagating
Cr.Le (μm)	66.6	272.8	242	252.6	330.9
S.D.	44.9	67.2	65.8	177.5	131.9
Cr.Dn (No./ mm^2)	0.018	0.146	0.021	0.375	0.032
S.D.	0.024	0.032	0.047	0.14	0.023
Cr.S.Dn ($\mu\text{m}/\text{mm}^2$)	2.36	25.27	4.63	52.24	11.8
S.D.	2.43	7.73	16.7	14.2	11.25

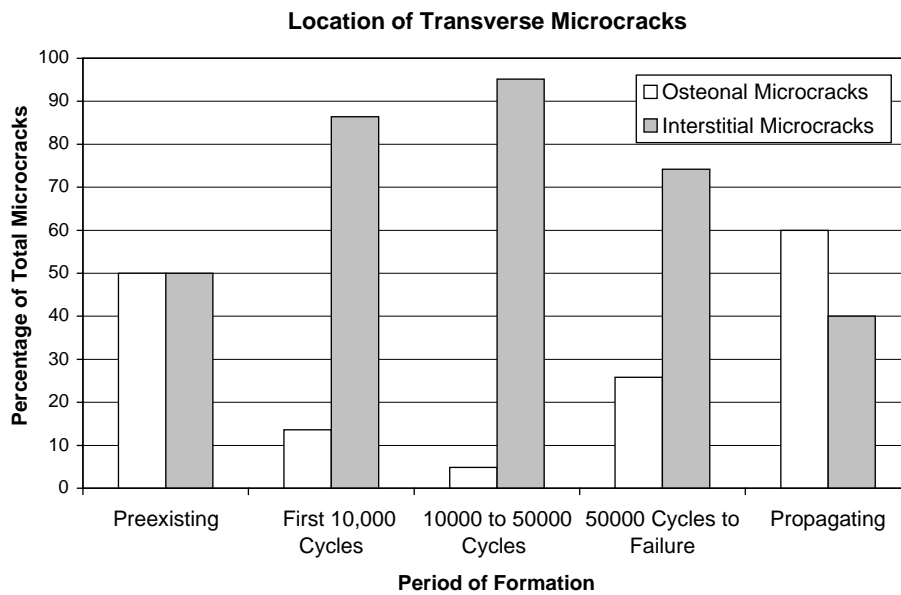


Fig. 4. Location of transverse microcracks. The majority of microcracks are found in interstitial bone with the exception of propagating cracks where 60% of them were found to penetrate osteons showing that the longer the crack, the greater the chance of it penetrating an osteon and enhancing the possibility of it causing outright failure.

Table 4

Data obtained from analysis of pre-existing microcracks from transverse and longitudinal sections dividing them into in vivo and machine-induced microcracks.

Crack type	In vivo microcracks	Machine-induced microcracks
Cr.Le (μm)	65.8	61.6
S.D.	9.6	38.7
Cr.Dn (No./ mm^2)	0.014	0.040
S.D.	0.005	0.036
Cr.S.Dn ($\mu\text{m}/\text{mm}^2$)	0.9	3.4
S.D.	0.16	3.1

during testing. This technique has allowed us to obtain data which previously has not been available, on the changes in damage states of individual specimens and individual cracks during a fatigue test.

From the three tests carried out with four agents used, crack accumulation during the life of a test specimen was shown to follow a characteristic curve in which many cracks initiate early during the specimen's life (first 10,000 cycles) but then accumulation of more cracks is suppressed with only a slight increase occurring between 10,000 and 50,000 cycles before microcracks rapidly accumulate after 50,000 cycles eventually resulting in failure. Fig. 2 shows the microcrack densities as a function of time for all the tests carried out illustrating this trend. Some authors have mentioned the possibility of a microstructural barrier concept governing the fatigue behaviour of bone (Martin and Burr, 1989; Taylor and Prendergast, 1997; Taylor, 1998; Akkus and Rimnac, 2001) with the bone's microstructure allowing microcracks to initiate rapidly but because of the morphology of osteonal bone, microcracks encounter barriers which suppress further growth. Fig. 4 adds further evidence to back up this theory: The vast majority of microcracks formed during the first 50,000 cycles of tests were located in interstitial bone indicating the difficulty of microcrack growth through or within osteons. In microcracks formed between 50,000 cycles and failure, this figure drops with 25% of microcracks being found in osteons. This suggests that later in a specimen's life, there is a greater potential for a microcrack to break through a cement line surrounding a secondary osteon, these cracks being longer and having more energy. A small percentage of microcracks which were classified as interstitial actually encountered cementlines surrounding osteons but were deflected and continued to grow. It may be useful to look at, in more depth, the differences between these microcracks and those which actually penetrate cementlines surrounding secondary osteons. Further work is presently ongoing in our laboratory studying this interaction.

Longitudinal lengths were found to be similar to those recorded by Burr and Martin (1993); the mean length was $296 \pm 257 \mu\text{m}$. Transverse lengths and densities were also similar to those found in other studies, (Schaffler et al., 1989; Burr and Stafford, 1990; Lee et al., 1998). It

is not surprising that cracks were longer in the longitudinal direction; the same occurs in composite materials when crack growth is relatively easy in one direction and difficult in the orthogonal one, due to the anisotropy of the material. It is also consistent with the prediction by Taylor and Lee (1998) who used the methods of stereology to estimate three-dimensional sizes and shapes using data from two-dimensional sections in the transverse and longitudinal planes.

At all stages during a specimens life, a higher density of microcracks was found in transverse sections than in longitudinal sections. At failure, the overall crack density in transverse sections was $\text{Cr.Dn.} = 0.80 \pm 0.17$ cracks/ mm^2 , the corresponding value for longitudinal sections was $\text{Cr.Dn.} = 0.56 \pm 0.14$ cracks/ mm^2 . As microcracks are longer in the longitudinal direction, any transverse cut through a section would be more likely to cut through a microcrack than a longitudinal cut of the same size. Only 6% of all microcracks detected were labelled with alizarin indicating that they existed prior to testing. Only one of this total of 54 pre-existing microcracks was found to propagate during testing and the specimen containing this crack did not have a shorter life than the mean, suggesting that in vivo or machine-induced microcracks did not affect the fatigue behaviour of these specimens. However, this may simply be a statistical effect, since propagating cracks make up such a small number of the total. From the control study carried out it was found that only 25.9% of all pre-existing cracks were in vivo cracks. This crack density is low in comparison to in vivo crack densities found in human bone (Burr and Stafford, 1990; Lee et al., 1998; O'Brien et al., 2000) but this is unsurprising as the bone samples were taken from young cattle (2–3 years old) and would be expected to be repaired in vivo very quickly. However, this also shows that less than 5% of all identified microcracks were formed by the machining process. This data validates the specimen manufacture and test technique used as it has often been suggested that the use of a CNC lathe in specimen manufacture leads to much larger amounts of artefactual damage than other machining techniques.

The great majority of microcracks (92%) were labelled with only one agent showing that they did not propagate between different stages of testing. No

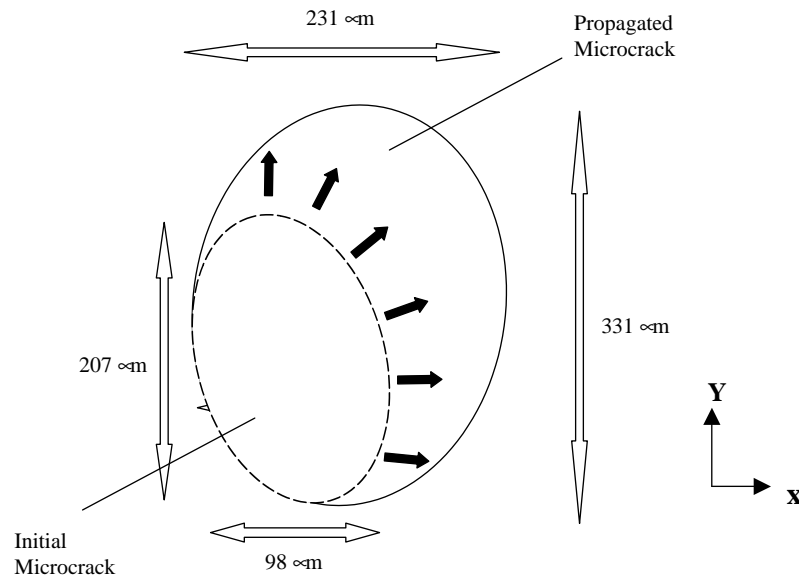


Fig. 5. Schematic of microcrack growth in two dimensions from mean transverse and longitudinal lengths obtained for microcracks formed in the first 50,000 cycles of testing and microcracks which were shown to propagate. Longitudinal microcracks are those in the Y -plane while transverse microcracks are those found in the X -plane.

significant amount of microcrack coalescence was observed during testing so it would seem that most cracks are not dangerous and will never grow to cause failure. In trying to understand the fatigue behaviour of bone, our attention should focus on the small percentage of cracks which do propagate, and so are potentially dangerous. Fig. 5 portrays this and attempts to show how an individual microcrack may develop as the test progresses. This shows a microcrack propagating in only one direction in both the transverse plane (i.e. “eastwards”) and in one direction longitudinally (i.e. “northwards”) to reflect our observations. This example shows that cracks are longer in the longitudinal direction than in the transverse direction at both stages of growth. Propagation did not take place from both ends of a microcrack. This one-sided growth may be explained as follows, secondary osteons in bone run parallel to the longitudinal axis of longbones. If the microcrack shown above were lying between two adjacent osteons, as the microcrack grew in size it would most likely break through the cement line of whichever osteon was weakest and continue to grow in that direction preferentially.

The technique used in this study to obtain ground sections is the most commonly used technique to study microcracks in bone. It gives accurate results of microcrack densities, but does not give very accurate information of microcrack lengths unless (as in this study) a large sample size is used, because for every 100–150 μm section obtained, 200–300 μm of bone are wasted in the cutting and grinding processes. Furthermore, it does not provide information on the shapes and sizes of individual microcracks. For example, if 100 transverse

slices were cut through the “virtual” microcrack in Fig. 5, 37% of the slices would go through the second part of the microcrack only, i.e. be labelled only with calcein. So by the classification used, these 37 sections would be classified as non-propagating microcracks formed after 50,000 cycles had elapsed when in fact they are actually sections through a propagating microcrack but have gone through a part of the crack containing only one agent. If the plane at which the sections are cut is changed, even more than 37% of sections may be labelled with only one agent and misclassified. So, although only 8% of all microcracks were shown to propagate in this study, it would be expected that this would be an underestimate of the actual number of propagating microcracks by approximately a factor of 2.

This work has generated new data on the process by which microcracks grow in compact bone and supports the concept of a microstructural barrier effect existing and having a major effect on the fatigue behaviour of bone.

Acknowledgements

This work was funded by the Health Research Board of Ireland, Cappagh Hospital Trust and the Research Committee of the Royal College of Surgeons in Ireland.

References

- Akkus, O., Rimnac, C.M., 2001. Cortical bone tissue resists fatigue fracture by deceleration and arrest of microcrack growth. *Journal of Biomechanics* 34, 757–764.

- Burr, D.B., Martin, R.B., 1993. Calculating the probability that microcracks initiate resorption spaces. *Journal of Biomechanics* 26, 613–616.
- Burr, D.B., Martin, R.B., Schaffler, M.B., Radin, E.L., 1985. Bone remodeling in response to in vivo fatigue microdamage. *Journal of Biomechanics* 18, 189–200.
- Burr, D.B., Stafford, T., 1990. Validity of the bulk-staining technique to separate artifactual from in vivo bone microdamage. *Clinical Orthopaedics and Related Research* 260, 305–308.
- Burr, D.B., Turner, C.H., Naick, P., Forwood, M.R., Ambrosius, W., Sayeed Hasan, M., Pidaparti, R.M.V., 1998. Does microdamage accumulation affect the mechanical properties of bone? *Journal of Biomechanics* 31, 337–345.
- Boyce, T.M., Fyhrie, D.P., Glotkowski, M.C., Radin, E.L., Schaffler, M.B., 1998. Damage type and strain mode associations in human compact bone bending fatigue. *Journal of Orthopaedic Research* 16, 322–329.
- Forwood, M.R., Parker, A.W., 1989. Microdamage in response to repetitive torsional loading in the rat tibia. *Calcified Tissue International* 45, 47–53.
- Frasca, P., 1981. Scanning electron microscopy studies of ground substance in the cement lines, resting lines, hypercalcified rings and reversal lines of human cortical bone. *Acta Anatomica* 109, 115–121.
- Jepsen, K.J., Davy, D.T., Krzyzpow, D.J., 1999. The role of the lamellar interface during torsional yielding of human cortical bone. *Journal of Biomechanics* 32, 303–310.
- Lee, T.C., Arthur, T.L., Gibson, L.J., Hayes, W.C., 2000aa. Sequential labelling of microdamage in bone using chelating agents. *Journal of Orthopaedic Research* 18, 322–325.
- Lee, T.C., Myers, E.R., Hayes, W.C., 1998. Fluorescence-aided detection of microdamage in compact bone. *Journal of Anatomy* 193, 179–184.
- Lee, T.C., O'Brien, F.J., Taylor, D., 2000bb. The nature of fatigue damage in bone. *International Journal of Fatigue* 22, 847–853.
- Lee, T.C., Taylor, D., 1999. Bone remodelling: should we cry Wolff? *Irish Journal of Medical Science* 168, 102–105.
- Martin, R.B., 2000. Toward a unifying theory of bone remodelling. *Bone* 26, 1–6.
- Martin, R.B., Burr, D.B., 1982. A hypothetical mechanism for the stimulation of osteonal remodelling by fatigue damage. *Journal of Biomechanics* 15, 137–139.
- Martin, R.B., Burr, D.B., 1989. *The structure, function and adaption of cortical bone*. Raven Press, New York.
- Mori, S., Burr, D.B., 1993. Increased intracortical remodeling following fatigue damage. *Bone* 14, 103–109.
- O'Brien, F.J., Taylor, D., Dickson, G.R., Lee, T.C., 2000. Visualisation of three-dimensional microcracks in compact bone. *Journal of Anatomy* 197, 413–420.
- O'Brien, F.J., Taylor, D., Lee, T.C., 2002. An improved labelling technique for monitoring microcrack growth in compact bone. *Journal of Biomechanics* 35, 523–526.
- Park, H.C., Lakes, R.S., 1986. Cosserat micromechanics of human bone: strain redistribution by a hydration sensitive constituent. *Journal of Biomechanics* 19, 385–397.
- Prendergast, P.J., Taylor, D., 1994. Prediction of bone adaptation using damage accumulation. *Journal of Biomechanics* 8, 1067–1076.
- Schaffler, M.B., Choi, K., Milgrom, C., 1994aa. Microcracks and aging in human femoral compact bone. *Proceedings of the Orthopaedic Research Society* 19, 190.
- Schaffler, M.B., Choi, K., Milgrom, C., 1995. Aging and matrix microdamage accumulation in human compact bone. *Bone* 17, 521–525.
- Schaffler, M.B., Pitchford, W., Choi, K., Riddle, J.M., 1994bb. Examination of compact bone microdamage using back-scattered electron microscopy. *Bone* 15, 483–488.
- Schaffler, M.B., Radin, E.L., Burr, D.B., 1989. Mechanical and morphological effects of strain rate on fatigue in compact bone. *Bone* 10, 207–214.
- Taylor, D., 1998. Microcrack growth parameters for compact bone deduced from stiffness variations. *Journal of Biomechanics* 31, 587–592.
- Taylor, D., Lee, T.C., 1998. Measuring the shape and size of microcracks in bone. *Journal of Biomechanics* 31, 1177–1180.
- Taylor, D., Prendergast, P.J., 1997. A model for fatigue crack propagation and remodelling in compact bone. *Journal of Engineering in Medicine* 211, 369–375.
- Taylor, D., O'Brien, F.J., Prina Mello, A., Ryan, C., O'Reilly, P., Lee, T.C., 1999. Compression data on bovine bone confirms that 'stressed volume' principle explains the variability of fatigue strength results. *Journal of Biomechanics* 32, 1199–1203.
- Ziopoulos, P., Currey, J.D., Sedman, A.J., 1994. An examination of the micromechanics of failure in bone and antler by acoustic emission tests and laser scanning confocal microscopy. *Medical Engineering and Physics* 16, 203–212.